NUMERICAL AND BIFURCATIONS ANALYSIS FOR MULTI-ORDER FRACTIONAL MODEL OF HIV INFECTION OF CD4$^+$T-CELLS

Mohsen ALIPOUR[1], Sadia ARSHAD[2], Dumitru BALEANU[3]

In this paper, we solve the dynamical system of HIV infection of CD4+ T-cells within the multi-order fractional derivatives. The Bernstein operational matrices in arbitrary interval $[a,b]$ are applied to obtain the approximate analytical solution of the model. In this way, the fractional differential equations are reduced to an algebraic easily solvable system. The obtained solutions are accurate and the method is very efficient and simple in implementation. With the help of bifurcation analysis, we acquired the critical value of viral death rate, that is, if viral death rate is greater than the critical value then level of virus particles starts to decline and thus free virus will eventually eliminate and patient is cured. Further, we found the threshold for viral infection rate analytically, which assures the stability of uninfected equilibrium and virus will ultimately eradicate.

Keywords: HIV infection of CD4$^+$T-cells, Operational matrices, Bernstein polynomials, Caputo fractional derivative, Bifurcation analysis.

1. Introduction

Since the early 1980s, many mathematical models of HIV have been developed to understand relations of HIV and the human immune system. In this way the public health officials can better compare, plan, implement and evaluate several programs for prevention, treatment and control of this disease. We refer the reader to excellent review paper on differential equation models of HIV on different phenomena [1]. Quantitative analysis of HIV-1 replication in vivo has made significant contributions to understanding of AIDS pathogenesis and antiretroviral treatment ([2, 3]). Detailed mathematical analysis on such models, we refer to the survey papers [4] and [5]. In [6] a dynamic model was introduced by dissemination of virus HIV in the bloodstream. This model contains free virus, latently infected CD4$^+$T-cells, actively infected CD4$^+$T-cells and uninfected CD4$^+$T-cells. The cell membranes of biological organism are set in class of models with non-integer order, since it has been proved that they have fractional-

[1] Department of Mathematics, Faculty of Basic Science, Babol Noshirvani University of Technology, P.O. Box 47148-71167, Babol, Iran, email: m.alipour2323@gmail.com, m.alipour@nit.ac.ir
[2] Academy of Mathematics and Systems Science, Chinese Academy of Sciences, Beijing, China, s.arshad.pak@gmail.com
[3] Cankaya University, dumitru@cankaya.edu.tr

order electrical conductance [7]. The greatest success in the rheology was obtained when the fractional derivatives were applied for the cell rheological behavior [8]. Furthermore, in [9] we can see that the model of treatment of brainstem vestibule-oculomotor neurons with fractional order gives better results than the classical one. Also, many fractional models are used in biological systems since they are very close to fractals [10]. Recently, many works have done on modeling the HIV infection with integer and fractional orders of derivatives [11-17]. In this study, we focus on the multi-order fractional of HIV infection of CD4$^+$T-cells as follows:

$$\begin{cases} {}_0^c D_t^{\alpha} \mathrm{T}(t) = s - \mu_{\mathrm{T}} \mathrm{T}(t) + r\mathrm{T}(t)\left(1 - \dfrac{\mathrm{T}(t)+\mathrm{I}(t)}{\mathrm{T}_{\max}}\right) - k_1 V(t)\mathrm{T}(t), \\ {}_0^c D_t^{\beta} \mathrm{I}(t) = k_2 V(t)\mathrm{T}(t) - \mu_I \mathrm{I}(t), \\ {}_0^c D_t^{\gamma} V(t) = N\mu_b \mathrm{I}(t) - k_1 V(t)\mathrm{T}(t) - \mu_V V(t), \end{cases} \tag{1}$$

with the following initial conditions

$$\mathrm{T}(0) = \frac{\mathrm{T}_{\max}\left(r - \mu_T + \sqrt{(r-\mu_T)^2 + \dfrac{4rs}{\mathrm{T}_{\max}}}\right)}{2r}, \quad \mathrm{I}(0) = 0, \quad V(0) = V_0, \tag{2}$$

where the notations are defined as follows:

$\mathrm{T}(t)$: Concentration of healthy CD4$^+$T-cells at time t.

$\mathrm{I}(t)$: Concentration of infected CD4$^+$T-cells at time t.

$V(t)$: Concentration of free HIV at time t.

We note that every lysing cell releases N viral particles, so $N\mu_b$ is the source for free virus. Moreover, in general we have $r > \mu_T$ and $\mu_T \mathrm{T}_{\max} > s$.

We applied the Bernstein operational matrices (BOM) to obtain the approximate analytical solution of (1) keeping in mind that the Bernstein polynomials (BPs) were used successfully for solving many problems in various fields of mathematics, physics and engineering [18-22].

The structure of the paper is as follows: In Section 2, we introduced some basic concepts of the fractional calculus and BPs. In Section 3, we presented the operational matrix of Caputo fractional derivative by BPs in the interval $[a,b]$. In Section 4, we used BOM for solving the multi-order fractional of HIV infection of CD4$^+$T-cells. Bifurcation analysis of HIV model is given in section 5. In section 6, the numerical simulation proved the applicability and accuracy of the presented method. The conclusions of our work are reported in the final section.

2. Primary concepts

Below we present some basic concepts used in this manuscript.

Definition 2.1. [23] The definition of the Riemann-Liouville fractional integral operator and Caputo fractional derivative of order $\alpha \geq 0$ for function $y(t)$ are given below, namely

$$\begin{aligned} &{}_aI_t^{\alpha} y(t) = \frac{1}{\Gamma(\alpha)} \int_a^t (t-\tau)^{\alpha-1} y(\tau)\, d\tau, \quad \alpha > 0,\ t > a, \\ &{}_aI_t^{0} y(t) = y(t), \end{aligned} \tag{3}$$

$${}_a^C D_t^{\alpha} y(t) = \begin{cases} \dfrac{1}{\Gamma(n-\alpha)} \int_a^t (t-\tau)^{n-\alpha-1} y^{(n)}(\tau)\, dx & n-1 < \alpha < n, \\ \dfrac{d^n y(t)}{dt^n} & \alpha = n. \end{cases} \tag{4}$$

Lemma 2.2. Le $\beta_{i,m}(t) = \binom{m}{i} \dfrac{(t-a)^i (b-t)^{m-i}}{(b-a)^m}$, $i = 0,1,\cdots,m$ are the Bernstein polynomials of degree m on interval $[a,b]$ and

$\bar{T}_m(t) = \left[1, (t-a), (t-a)^2, \ldots, (t-a)^m\right]^T$, $\Psi_m(t) = \left[\beta_{0,m}(t), \beta_{1,m}(t), \cdots, \beta_{m,m}(t)\right]^T$,

then

$$\Psi_m(t) = A\, \bar{T}_m(t), \tag{5}$$

where $A = \left(a_{i,j}\right)_{i,j=1}^{m+1}$ and

$$a_{i+1,j+1} = \begin{cases} \dfrac{(-1)^{j-i}}{(b-a)^j} \binom{m}{i} \binom{m-i}{j-i} & i \leq j, \\ 0 & i > j, \end{cases} \qquad i, j = 0,1,\ldots,m.$$

Proof. From the expansion of $(b-x)^{m-i}$, we get

$$\beta_{i,m}(t) = \binom{m}{i} \frac{(t-a)^i (b-t)^{m-i}}{(b-a)^m} = \binom{m}{i} \frac{(t-a)^i ((b-a)+(a-t))^{m-i}}{(b-a)^m} =$$

$$\binom{m}{i} \frac{(t-a)^i}{(b-a)^m} \left(\sum_{k=0}^{m-i} \binom{m-i}{k} (b-a)^{m-i-k} (a-t)^k \right) = \sum_{k=0}^{m-i} (-1)^k \binom{m}{i} \binom{m-i}{k} \left(\frac{t-a}{b-a} \right)^{k+i}$$

$$= \sum_{j=i}^{m} (-1)^{j-i} \binom{m}{i} \binom{m-j}{j-i} \left(\frac{t-a}{b-a} \right)^j, \quad i = 0,1\ldots,m.$$

then, we can conclude that $\Psi_m(t) = A\, \bar{T}_m(t)$. □

For any function $y \in C^{m+1}[a,b]$ we can approximate $y(t)$ as follows [19]

$$y(t) \approx \sum_{i=0}^{m} c_i \beta_{i,m}(t) = c^T \Psi_m(t), \tag{6}$$

where $c^T = [c_0, c_2, \cdots, c_m]$ is obtained as

$$C^T = \left(\int_a^b y(t) \Psi_m(t)^T dt \right) Q^{-1}, \quad Q = \left(Q_{i,j} \right)_{i,j=1}^{m+1} \text{ and}$$

$$Q_{i+1,j+1} = \int_a^b \beta_{i,m}(t) \beta_{j,m}(t) dx = \frac{(b-a)\binom{m}{i}\binom{m}{j}}{(2m+1)\binom{2m}{i+j}}, \quad i,j = 0,1,\cdots m. \tag{7}$$

Definition 2.3. We denote the operational matrix of product for vector c based on basis $\Psi_m(t)$ by $\hat{C}$ and define it as:

$$c^T \Psi_m(t) \Psi_m(t)^T \approx \Psi_m(t)^T \hat{C}. \tag{8}$$

In order to get $\hat{C}$, we can follow the steps below.

By using (5) we obtain

$$\begin{aligned} c^T \Psi_m(t) \Psi_m(t)^T &= c^T \Psi_m(t) \left(\overline{T}_m(t)^T A^T \right) \\ &= \left[c^T \Psi_m(t), (t-a)\left(c^T \Psi_m(t) \right), \ldots, (t-a)^m \left(c^T \Psi_m(t) \right) \right] A^T \\ &= \left[\sum_{i=0}^{m} c_i \beta_{i,m}(t), \sum_{i=0}^{m} c_i (t-a) \beta_{i,m}(t), \ldots, \sum_{i=0}^{m} c_i (t-a)^m \beta_{i,m}(t) \right] A^T. \end{aligned}$$

Then, we can apply the approximation

$$(t-a)^k \beta_{i,m}(t) \approx e_{k,i} \Psi_m(t), \ (i,k = 0,1,\ldots,m), \ e_{k,i} = \left[e_{k,i}^0 \ , \ e_{k,i}^1 \ , \ \ldots \ , \ e_{k,i}^m \right]^T,$$

such that

$$e_{k,i} = \frac{Q^{-1}\binom{m}{i}(b-a)^{k+1}}{2m+k+1} \left[\frac{\binom{m}{0}}{\binom{2m+k}{i+k}}, \frac{\binom{m}{1}}{\binom{2m+k}{i+k+1}}, \ldots, \frac{\binom{m}{m}}{\binom{2m+k}{i+k+m}} \right]^T, \qquad i,k = 0,1,\ldots,m.$$

So, we get

$$\sum_{i=0}^{m} c_i\,(t-a)^k\,\beta_{i,m}(t) \approx \sum_{i=0}^{m} c_i \left(\sum_{j=0}^{m} e_{k,i}^{j}\,\beta_{j,m}(t) \right) = \sum_{i=0}^{m} \beta_{j,m}(t) \left(\sum_{i=0}^{m} c_i\, e_{k,i}^{j} \right)$$

$$= \Psi_m(t)^T \left[\sum_{i=0}^{m} c_i e_{k,i}^{0}, \sum_{i=0}^{m} c_i e_{k,i}^{1}, \ldots, \sum_{i=0}^{m} c_i e_{k,i}^{m} \right]^T$$

$$= \Psi_m(t)^T \underbrace{\left[e_{k,0}, e_{k,1}, \ldots, e_{k,m} \right]}_{V_k} c = \Psi_m(t)^T V_k\, c.$$

Finally, by the above results, we write

$$c^T \Psi_m(t)\, \Psi_m(t)^T \approx \Psi_m(t)^T \underbrace{\left[V_0\, c, V_1\, c, \ldots, V_m\, c \right]}_{\hat{C}} A^T,$$

therefore $\hat{C}$ is obtained.

3. BOM of Caputo fractional derivative

Now, the aim is to get the BOM of fractional derivative. Thus, we write:

$$\begin{aligned} {}_a^C D_t^{\alpha} \Psi_m(t) &= \frac{1}{\Gamma(n-\alpha)} \int_a^t (t-\tau)^{n-\alpha-1} \frac{d^n \Psi_m(\tau)}{d\tau^n} d\tau \\ &= \frac{1}{\Gamma(n-\alpha)} \int_a^t (t-\tau)^{n-\alpha-1} A \frac{d^n \bar{T}_m(\tau)}{d\tau^n} d\tau \\ &= A \left[{}_a^C D_t^{\alpha} 1, {}_a^C D_t^{\alpha} (t-a), \ldots, {}_a^C D_t^{\alpha} (t-a)^m \right]^T \\ &= AW\, T_{m,\alpha}(t), \end{aligned}$$

where $W = diag\left(w_{0,0}, w_{1,1}, \ldots, w_{m,m} \right)$ and $T_{m,\alpha}$ are as follows:

$$w_{j,j} = \begin{cases} 0 & j = 0, \ldots, n-1, \\ \dfrac{j!}{\Gamma(j+1-\alpha)} & j = n, \ldots, m, \end{cases}$$

$$T_{m,\alpha}(t) = \left[\underbrace{0, \ldots, 0}_{n\ times}, (t-a)^{n-\alpha}, \ldots, (t-a)^{m-\alpha} \right]^T.$$

Now, we need to approximate $(t-a)^{i-\alpha}$ $(i = n, \ldots, m)$ based on BPs by applying (6). So, we get

$$(t-a)^{i-\alpha} \approx E_i^T \Psi_m(t),$$

where

$$E_i = \frac{(b-a)^{i-\alpha+1} m!}{\Gamma(i+m-\alpha+2)} Q^{-1} \left[\frac{\Gamma(i-\alpha+1)}{0!}, \frac{\Gamma(i+1-\alpha+1)}{1!}, \ldots, \frac{\Gamma(i+m-\alpha+1)}{m!} \right]^T,$$
$$i = n, \ldots, m.$$

Then, we write

$${}_a^C D_t^\alpha \Psi_m(t) \approx \underbrace{AW \left[\underbrace{0, \ldots, 0}_{n \text{ times}}, E_n, \ldots, E_m \right]^T}_{D_\alpha} \Phi_m(t).$$

Finally, we conclude that

$${}_a^C D_t^\alpha \Psi_m(t) \approx D_\alpha \ \Psi_m(t). \tag{9}$$

We denote the BOM of Caputo fractional derivative of order α by D_α.

4. BOM for solving THE PROPOSED MODEL

By using (6), we apply the following approximations:

$$\mathrm{T}(t) \approx \tilde{\mathrm{T}}^T \Psi_m(t), \qquad \mathrm{I}(t) \approx \tilde{\mathrm{I}}^T \Psi_m(t), \qquad V(t) \approx \tilde{V}^T \Psi_m(t). \tag{10}$$

Then, by taking into account (9) and (10) we obtain

$$\begin{aligned}
&{}_0^C D_t^\alpha \mathrm{T}(t) \approx {}_0^C D_t^\alpha \left(\tilde{\mathrm{T}}^T \Psi_m(t) \right) = \tilde{\mathrm{T}}^T \, {}_0^C D_t^\alpha \Psi_m(t) \approx \tilde{\mathrm{T}}^T D_\alpha \Psi_m(t), \\
&{}_0^C D_t^\beta \mathrm{I}(t) \approx {}_0^C D_t^\beta \left(\tilde{\mathrm{I}}^T \Psi_m(t) \right) = \tilde{\mathrm{I}}^T \, {}_0^C D_t^\beta \Psi_m(t) \approx \tilde{\mathrm{I}}^T \Psi_\beta \Psi_m(t), \\
&{}_0^C D_t^\gamma V(t) \approx {}_0^C D_t^\gamma \left(\tilde{V}^T \Psi_m(t) \right) = \tilde{V}^T \, {}_0^C D_t^\gamma \Psi_m(t) \approx \tilde{V}^T D_\gamma \Psi_m(t).
\end{aligned} \tag{11}$$

We observe that from (10) and (11), the problems (1) and (2) are reduced to

$$\begin{cases}
\tilde{\mathrm{T}}^T D_\alpha \Psi_m(t) = s1^T \Psi_m(t) - \mu_T \tilde{\mathrm{T}}^T \Psi_m(t) + r \tilde{\mathrm{T}}^T \Psi_m(t) \\
-\dfrac{r}{T_{\max}} \left(\tilde{\mathrm{T}}^T \Psi_m(t) \Psi_m(t)^T \tilde{\mathrm{T}} + \tilde{\mathrm{T}}^T \Psi_m(t) \Psi_m(t)^T \tilde{\mathrm{I}} \right) - k_1 \tilde{V}^T \Psi_m(t) \Psi_m(t)^T \tilde{\mathrm{T}}, \\
\tilde{\mathrm{I}}^T D_\beta \Psi_m(t) = k_2 \tilde{\mathrm{T}}^T \Psi_m(t) \Psi_m(t)^T \tilde{V} - \mu_I \tilde{\mathrm{I}}^T \Psi_m(t), \\
\tilde{V}^T D_\gamma \Psi_m(t) = N \mu_b \tilde{\mathrm{I}}^T \Psi_m(t) - k_1 \tilde{\mathrm{T}}^T \Psi_m(t) \Psi_m(t)^T \tilde{V} - \mu_V \tilde{V}^T \Psi_m(t),
\end{cases} \tag{12}$$

and

$$\begin{aligned}
&\tilde{\mathrm{T}}^T\Psi_m(0)=\frac{\mathrm{T}_{\max}\left(r-\mu_T+\sqrt{(r-\mu_T)^2+\dfrac{4rs}{\mathrm{T}_{\max}}}\right)}{2r},\\
&\tilde{\mathrm{I}}^T\Psi_m(0)=0,\quad \tilde{V}^T\Psi_m(0)=V_0.
\end{aligned}\tag{13}$$

Here $1=\left[\underbrace{1,1,\ldots,1}_{m+1\ times}\right]^T$, since $\sum_{i=0}^{m}\beta_{i,m}(t)=1^T\Psi_m(t)=1$. So, by the operational matrix of product in (8), we have

$$\begin{cases}
\tilde{\mathrm{T}}^T D_\alpha\Psi_m(t)=s1^T\Psi_m(t)+(r-\mu_T)\tilde{\mathrm{T}}^T\Psi_m(t)\\
\qquad\qquad -\dfrac{r}{\mathrm{T}_{\max}}\left(\Psi_m(t)^T\hat{\tilde{\mathrm{T}}}\tilde{\mathrm{T}}+\Psi_m(t)^T\hat{\tilde{\mathrm{T}}}\tilde{\mathrm{I}}\right)-k_1\Psi_m(t)^T\hat{\tilde{\mathrm{T}}}\tilde{V},\\
\tilde{\mathrm{I}}^T D_\beta\Psi_m(t)=k_2\Psi_m(t)^T\hat{\tilde{\mathrm{T}}}\tilde{V}-\mu_I\tilde{\mathrm{I}}^T\Psi_m(t),\\
\tilde{V}^T D_\gamma\Psi_m(t)=N\mu_b\tilde{\mathrm{I}}^T\Psi_m(t)-k_1\Psi_m(t)^T\hat{\tilde{\mathrm{T}}}\tilde{V}-\mu_V\tilde{V}^T\Psi_m(t),
\end{cases}\tag{14}$$

where $\hat{\tilde{\mathrm{T}}}$ is the operational matrix of product for $\tilde{\mathrm{T}}$ based on $\Psi_m(t)$. Thus we can write

$$\begin{cases}
\left(\tilde{\mathrm{T}}^T D_\alpha-s1^T-(r-\mu_T)\tilde{\mathrm{T}}^T+\dfrac{r}{\mathrm{T}_{\max}}\left(\tilde{\mathrm{T}}^T\hat{\tilde{\mathrm{T}}}^T+\tilde{\mathrm{I}}^T\hat{\tilde{\mathrm{T}}}^T\right)+k_1\tilde{V}^T\hat{\tilde{\mathrm{T}}}^T\right)\Psi_m(t)=0,\\
\left(\tilde{\mathrm{I}}^T D_\beta-k_2\tilde{V}^T\hat{\tilde{\mathrm{T}}}^T+\mu_I\tilde{\mathrm{I}}^T\right)\Psi_m(t)=0,\\
\left(\tilde{V}^T D_\gamma-N\mu_b\tilde{\mathrm{I}}^T+k_1\tilde{V}^T\hat{\tilde{\mathrm{T}}}^T+\mu_V\tilde{V}^T\right)\Psi_m(t)=0.
\end{cases}\tag{15}$$

Now, by applying the Tau method [24] for (15), we obtain the following algebraic equations:

$$\begin{cases} \int_0^b \left(\tilde{\mathrm{T}}^T D_\alpha - s\mathbf{1}^T - (r-\mu_T)\tilde{\mathrm{T}}^T + \frac{r}{\mathrm{T}_{\max}}\left(\tilde{\mathrm{T}}^T\hat{\tilde{\mathrm{T}}}^T + \tilde{\mathrm{I}}^T\hat{\tilde{\mathrm{T}}}^T\right) + k_1\tilde{V}^T\hat{\tilde{\mathrm{T}}}^T \right)\Psi_m(t)\beta_{i,m}(t)\,dt = 0, \\ \int_0^b \left(\tilde{\mathrm{I}}^T D_\beta - k_2\tilde{V}^T\hat{\tilde{\mathrm{T}}}^T + \mu_I\tilde{\mathrm{I}}^T \right)\Psi_m(t)\beta_{i,m}(t)\,dt = 0, \qquad i = 0,\ldots,m-1, \\ \int_0^b \left(\tilde{V}^T D_\gamma - N\mu_b\tilde{\mathrm{I}}^T + k_1\tilde{V}^T\hat{\tilde{\mathrm{T}}}^T + \mu_V\tilde{V}^T \right)\Psi_m(t)\beta_{i,m}(t)\,dt = 0. \end{cases}$$

(16)

Finally, the equations (16) with (13) produce a system of $3m+3$ algebraic equations and $3m+3$ variables which can be solved for $\tilde{\mathrm{T}}, \tilde{\mathrm{I}}$ and $\tilde{V}$, respectively. Finally, by making use of (10) we obtain the approximations for $\mathrm{T}(t), \mathrm{I}(t)$ and $V(t)$.

5. Bifurcation Analysis

In this section, we explore the long term behavior of HIV model. System (1) has two equilibrium points: the uninfected equilibrium $E_0 = (T_0, 0, 0)$ and the infected equilibrium $E^* = (T^*, I^*, V^*)$, where

$$T_0 = \frac{T_{max}}{2r}\left[r - \mu_T + \sqrt{(r-\mu_T)^2 + \frac{4sr}{T_{max}}} \right]$$

$$T^* = \frac{\mu_V\mu_I}{k_2N\mu_b - k_1\mu_I}, \quad I^* = \frac{k_2T^*V^*}{\mu_I}, \quad V^* = \frac{\mu_I[(s+(r-\mu_T)T^*)T_{max} - rT^{*2}]}{T^*[k_2rT^* + k_1\mu_IT_{max}]}.$$

The characteristic polynomial of Jacobian matrix at E_0 of linearized system of (1) is given by

$$(\lambda - A_1)(\lambda^2 + A_2\lambda + A_3) = 0$$

where $A_1 = r - \mu_T - \frac{2rT_0}{T_{max}} < 0.$; $A_2 = \mu_I + k_1T_0 + \mu_V$; $A_3 = \mu_I(k_1T_0 + \mu_V) - N\mu_bk_2T_0$.

It is easy to see that $\lambda_1 = A_1 < 0$. By Routh-Hurwitz Criteria E_0 is stable if and only if $A_2 > 0$ and $A_3 > 0$. Since A_2 is sum of positive elements, therefore $A_2 > 0$.

$$\begin{aligned} A_3 &= \mu_I(k_1T_0 + \mu_V) - N\mu_bk_2T_0 \\ &= \mu_I\left(\mu_V - \left(\frac{N\mu_bk_2T_0 - k_1T_0}{\mu_I}\right)\right) \\ &= \mu_I(\mu_V - \mu_{crit}) \end{aligned}$$

Where $\mu_{crit} = \frac{N\mu_b k_2 T_0 - k_1 T_0}{\mu_I}$

Hence, $\mu_V > \mu_{crit}$, implies $A_3 > 0$ which yields uninfected equilibrium point is asymptotically stable.

If $\mu_V = \mu_{crit}$, then $A_3 = 0$. This implies $\lambda_2 = 0 \; and \; \lambda_3 = -A_2 < 0$. Hence uninfected equilibrium point is stable when $\mu_V = \mu_{crit}$. If $\mu_V < \mu_{crit}$, then $A_3 < 0$ and we get $\lambda_2 = \frac{-A_2+\sqrt{A_2^2-4A_3}}{2} > 0 \; and \; \lambda_3 = \frac{-A_2-\sqrt{A_2^2-4A_3}}{2} < 0$.

Consequently uninfected equilibrium point is unstable when $\mu_V < \mu_{crit}$ as one eigenvalue is positive in this case.

From above analysis, we deduce that, μ_V is a bifurcation parameter for the uninfected steady state. Using parameter given in Table 1 and $N = 130$, we get $\mu_{V=}2.376$.

For μ_V< 2.376, the uninfected equilibrium is unstable, for μ_V>2.376 this equilibrium will become stable. Thus system (1) has a transcritical bifurcation at μ_V=2.376. Figure 1 represents the effect of change in μ_V on population of healthy CD4+ cells.

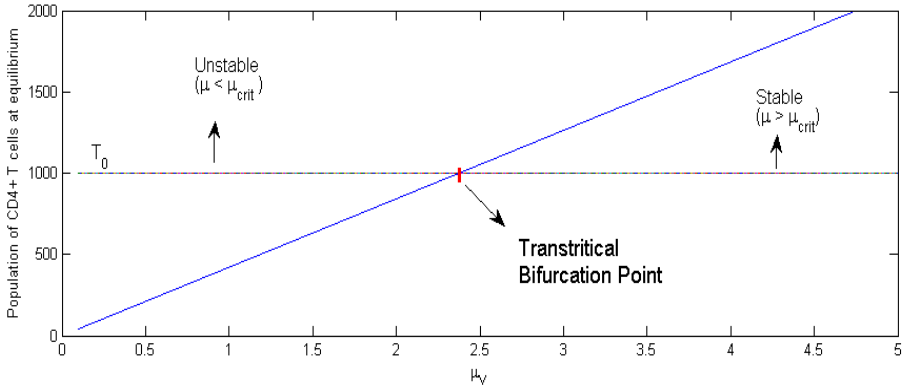

Fig. 1. Bifurcation diagram: Effect of viral death rate on T cells.

Following the similar analysis we acquire that k_1 (viral infection rate) is a bifurcation parameter which yields that system (1) is stable at E_0 if $k_1 > k_{crit}$, it will lose its stability at $k_1 = k_{crit}$ and it will turn out to be unstable if $k_1 < k_{crit}$, where $k_{crit} = \frac{N\mu_b k_2 T_0 - \mu_I \mu_V}{\mu_I}$.

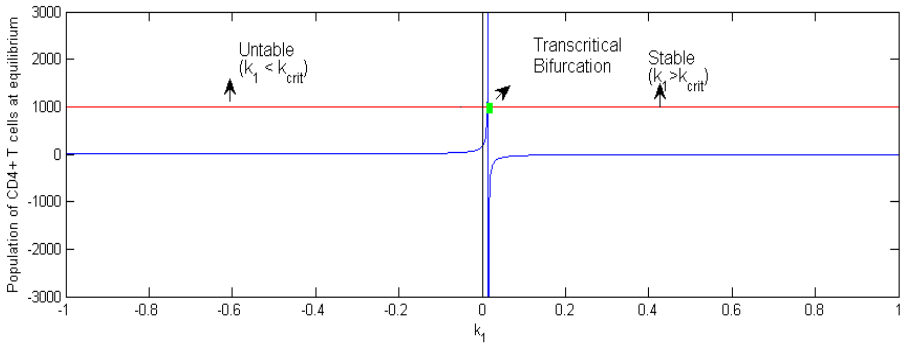

Fig. 2. Bifurcation diagram: Effect of viral infection rate on T cells.

Viral infection rate $k_{crit} = 0.0124$ for the parameter values given in Table 1 and $N = 800$. Fig. 2 illustrate the fact that E_0 is unstable if $k_1 < 0.0124$ and it will change its stability at $k_1 = 0.0124$ and become stable if $k_1 > 0.0124$.

6. Numerical simulation

In this section, we consider the parameter values given in Table 1. We utilize the presented method in the previous section for $m = 10$ and for different values of α, β, γ. Also, we can see the behaviors of $\mathrm{T}(t)$, $\mathrm{I}(t)$ and $V(t)$ for $\alpha = 1,\ \beta = \gamma = 0.9, 0.95, 1$ and $\beta = 1,\ \alpha = \gamma = 0.9, 0.95, 1$ and $\gamma = 1,\ \alpha = \beta = 0.9, 0.95, 1$ with $N = 1000$ in figures 3-5, respectively. Also, we display $\mathrm{T}(t)$, $\mathrm{I}(t)$ and $V(t)$ for $\alpha = 1,\ \beta = \gamma = 0.7, 0.8, 1$ and $\beta = 1,\ \alpha = \gamma = 0.7, 0.8, 1$ and $\gamma = 1,\ \alpha = \beta = 0.7, 0.8, 1$ with $N = 800$ in figures 6-8, respectively. The residuals of the obtained solutions for the problem (1) with $N = 800, 1000$ are plotted in figures 9-11.

Table 1.

Parameters used in the numerical simulations of model (1).

Parameter	Description	Value
s	Source of CD4$^+$T-cells from precursors	10 $mm^3 day^{-1}$
μ_T	Natural death rate of CD4$^+$T-cells	0.02 day^{-1}
μ_V	Death rate of free virus	2.4 day^{-1}
μ_b	Lytic death rate for infected cells	0.24 day^{-1}
r	Growth rate	0.03 day^{-1}
$\mathrm{T}_{\max}$	Carrying capacity	1500 mm^3
k_1	Rate of infection of T-cells for free virus	2.4×10^{-5} $mm^3 day^{-1}$
k_2	Rate of infection for cells actively infected	2×10^{-5} $mm^3 day^{-1}$
μ_I	A blanket death term of infected cells	0.26 day^{-1}
N	Number of virions produced by infected CD4$^+$T-cells	Varies

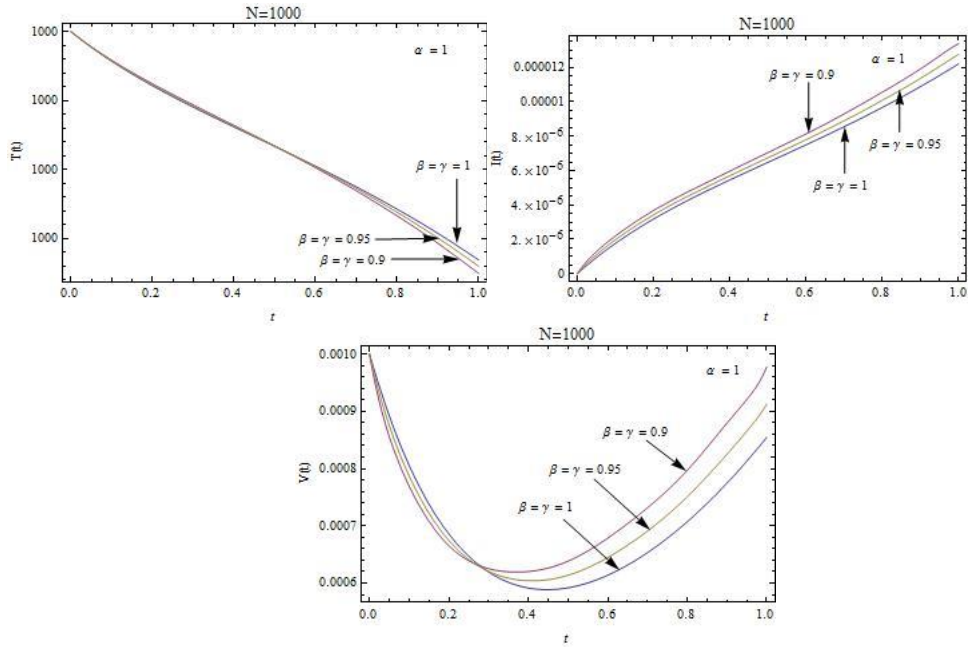

Fig. 3. Plot of $\mathrm{T}(t)$, $\mathrm{I}(t)$ and $V(t)$ for $N=1000$, $\alpha=1$, $\beta=\gamma=0.9,0.95,1$ and $m=10$.

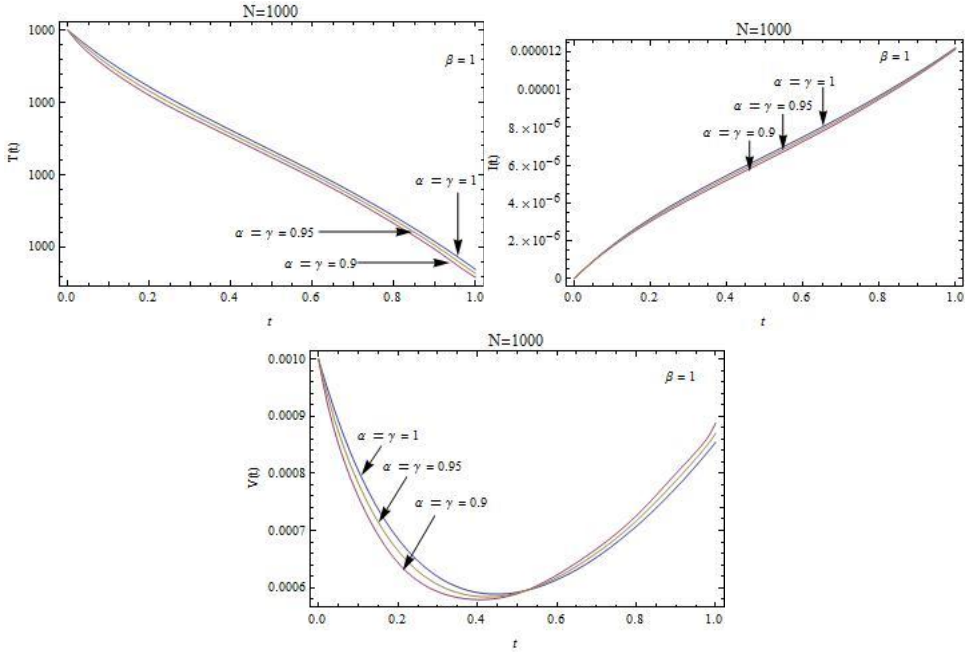

Fig. 4. Plot of $\mathrm{T}(t)$, $\mathrm{I}(t)$ and $V(t)$ for $N=1000$, $\beta=1$, $\alpha=\gamma=0.9,0.95,1$ and $m=10$.

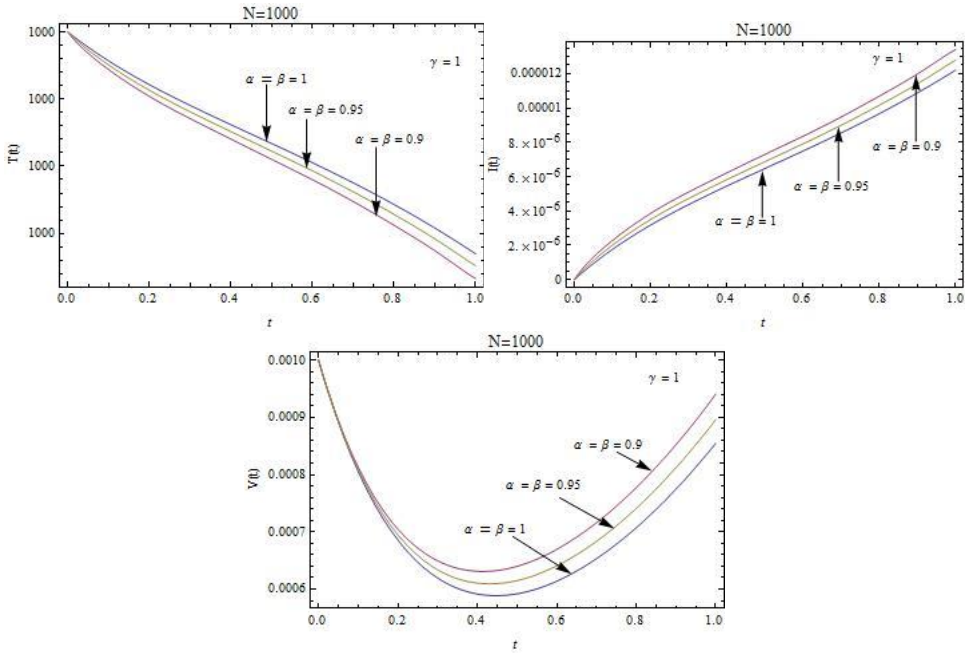

Fig. 5. Plot of $\mathrm{T}(t)$, $\mathrm{I}(t)$ and $V(t)$ for $N=1000$, $\gamma=1$, $\beta=\alpha=0.9,0.95,1$ and $m=10$.

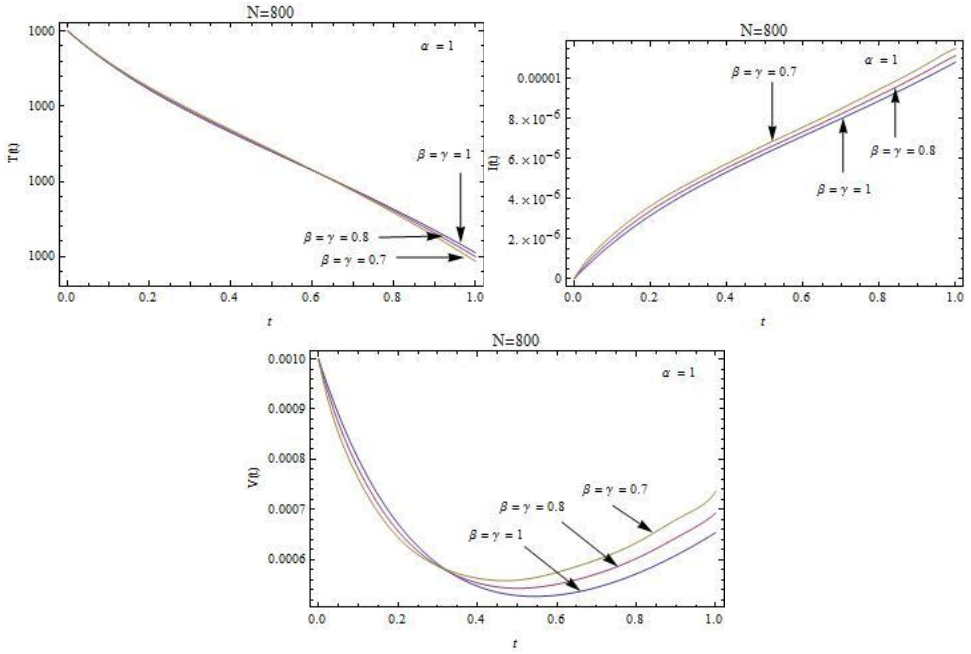

Fig. 6. Plot of $\mathrm{T}(t)$, $\mathrm{I}(t)$ and $V(t)$ for $N=800$, $\alpha=1$, $\beta=\gamma=0.7,0.8,1$ and $m=10$.

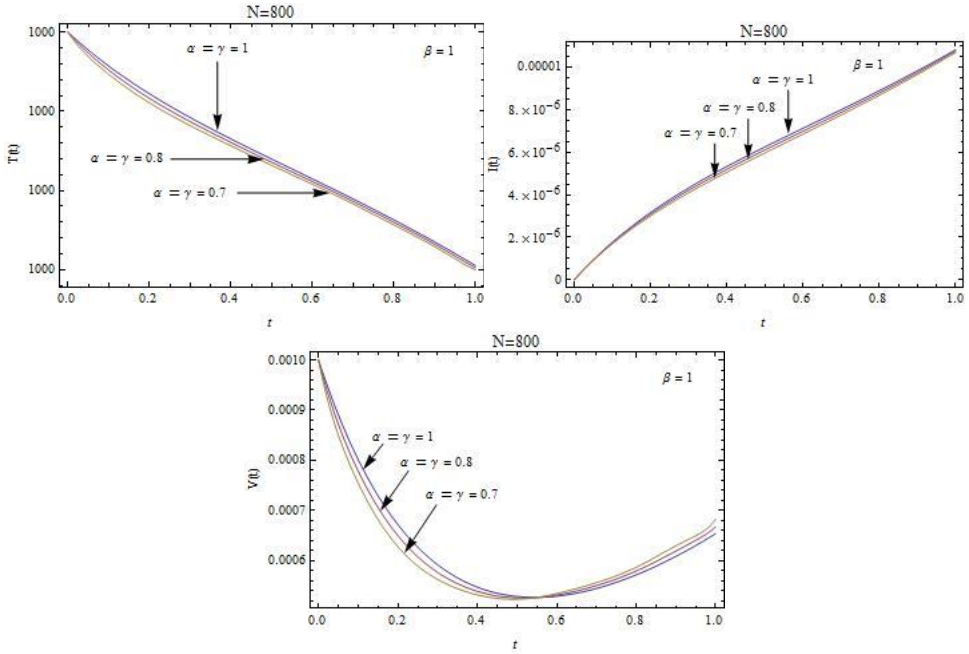

Fig. 7. Plot of $\mathrm{T}(t)$, $\mathrm{I}(t)$ and $V(t)$ for $N=800$, $\beta=1$, $\alpha=\gamma=0.7,0.8,1$ and $m=10$.

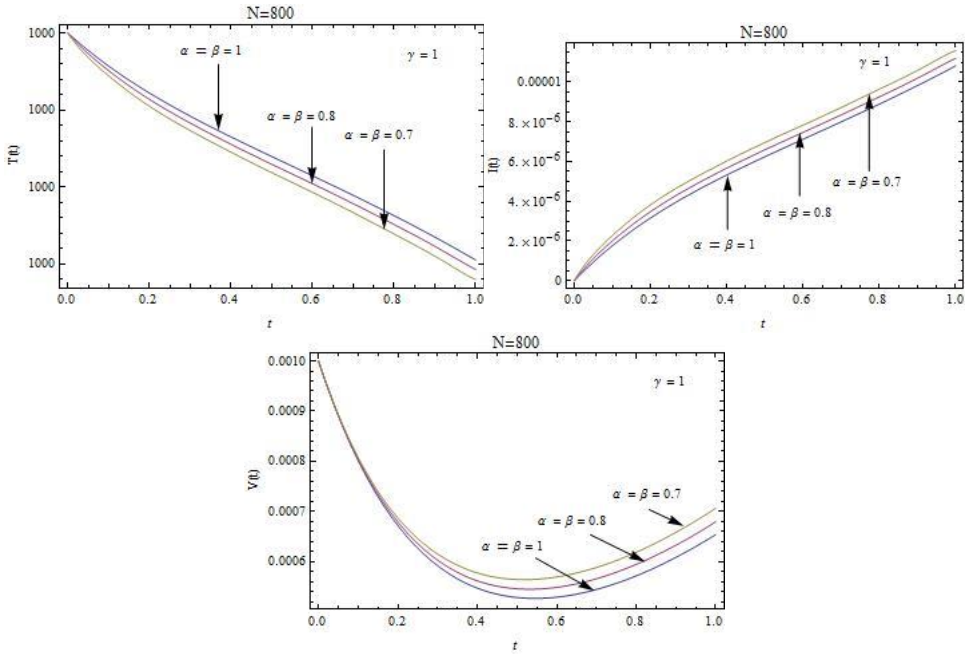

Fig. 8. Plot of $\mathrm{T}(t)$, $\mathrm{I}(t)$ and $V(t)$ for $N=800$, $\gamma=1$, $\alpha=\beta=0.7,0.8,1$ and $m=10$.

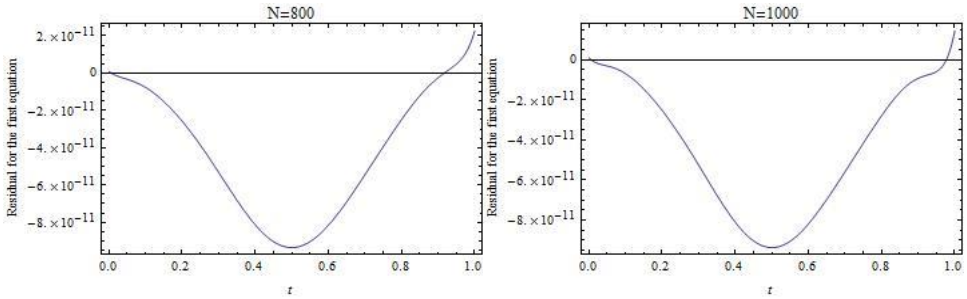

Fig. 9. Plot of the residual function for the first equation in (1) with $\alpha = \beta = \gamma = 1,\ m = 10$ and $N = 800, 1000$.

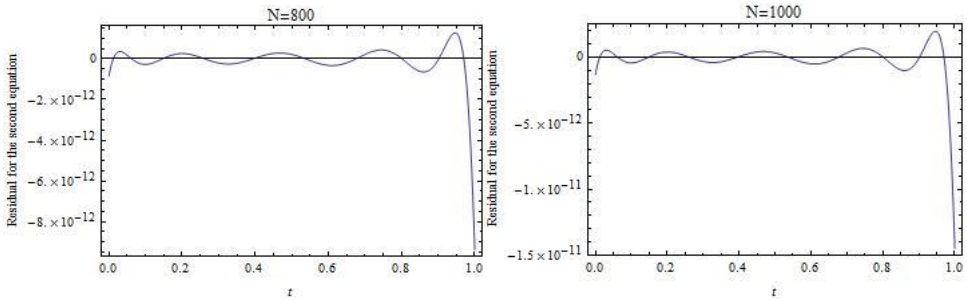

Fig. 10**.** Plot of the residual function for the second equation in (1) with $\alpha = \beta = \gamma = 1,\ m = 10$ and $N = 800, 1000$.

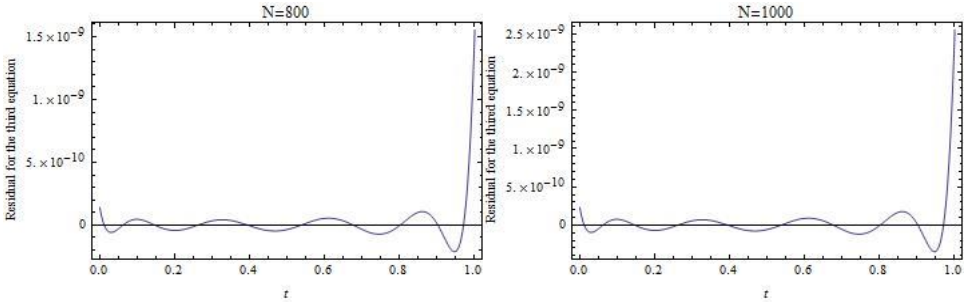

Fig**.** 11. Plot of the residual function for the third equation in (1) with $\alpha = \beta = \gamma = 1,\ m = 10$ and $N = 800, 1000$.

6. Conclusions

Human immunodeficiency virus (HIV) targets the CD4+ T lymphocytes commonly known as helper T cells. T-cells, like other lymphocytes, are formed in the bone marrow. Young cells transfer to the thymus, where they go through further differentiation and grown-up into immune capable T-cells. Although HIV attacking various kinds of cells, it inflicts the most disorder on the CD4+ T -cells by causing their destruction and decreasing the body's capability to struggle infection. In a clinical setting, the decline in the number of CD4+ T cells in blood and the blood ratio of CD4+/CD8+ T cells are both point toward the disease stage.

The number of T-cells in the blood in healthy persons is sustained comparatively constant, with CD4+ T cells consisting of about 1000 cells/mm^3.

In this work, we utilized BOM for solving the proposed multi-order fractional of HIV infection of CD4⁺T-cells. This method was applied for arbitrary interval [a,b], so we don't need to use variable changing for transfer the interval [a,b] to [0,1]. By using BOM, we reduced the initial nonlinear problem to an algebraic system that is easily solvable. In our model the non-local effects are better described by varying the values of α, β, γ. The reported numerical values of $\mathrm{T}(t)$, $\mathrm{I}(t)$ and $V(t)$ exhibit a strong dependence to the values of the fractional order as it can be seen from figures 1-6. When the orders of fractional derivative approach to 1, the classical solutions are recovered. Finally, we observe that the results have good accuracy and the presented method is very efficient to get approximate analytical solution of this problem.

Varying parameter values change the dynamical properties of HIV model. With the help of bifurcation analysis, we obtained the critical value μ_{crit} of viral death rate μ_V, that is, $\mu_V > \mu_{crit}$ cause reduction in level of virus and where as $\mu_V < \mu_{crit}$ implies diminution of CD4+ cells. Consequently, if virus lives long that if μ_V is declined then there is increased depletion of uninfected CD4+ cells, on the other hand if μ_V increase then virus will finally have eliminated. Viral infection rate k_1 play vital role in HIV dynamics, higher rate of viral infection might increase the reduction rate of uninfected T cells. We found the threshold k_{crit} for viral infection rate analytically, which shows that $k_1 = k_{crit}$ is a bifurcation point. Uninfected equilibrium will become stable as k_1 passes this point i.e. $k_1 > k_{crit}$ and patient is eventually cured.

REFERENCES

[1] *L. Rong, A. S. Perelson*, Modeling HIV persistence, the latent reservoir, and viralblips, Journal of Theoretical Biology 260 (2009) 308-331.

[2] *D. Finzi, R. Siliciano*, Viral dynamics in HIV-1 infection, Cell 93 (1998) 665-671.

[3] *A.S. Perelson*, Modelling viral and immune system dynamics, Nat. Rev. Immunol. 2 (2002) 2836.

[4] *A.S. Perelson, P.W. Nelson*, Mathematical analysis of HIV-1 dynamics in vivo, SIAM Rev. 41 (1999) 3-44.

[5] *D.E. Kirschner*, Using mathematics to understand HIV immune dynamics, Notices Am. Math. Soc. 43 (1996) 191-202.

[6] *A.S. Perelson, D.E. Kirschner, R. De Boer*, Dynamics of HIV infection of CD4⁺T -cells, Mathematical Bioscience,**114**, 81-125(1993).

[7] *K.S. Cole*, Electric conductance of biological systems, in: Proc. Cold Spring Harbor Symp. Quant. Biol, Cold Spring Harbor, New York, 1993, pp. 107-116.

[8] *V.D. Djordjevic, J. Jaric, B. Fabry, J.J. Fredberg, D. Stamenovi¢*, Fractional derivatives embody essential features of cell rheological behavior, Annals of Biomedical Engineering,**31,** 692-699(2003).

[9] *T.J. Anastasio*, The fractional-order dynamics of bainstem vestibulo-oculomotor neurons, Biological Cybernetics,**72,** 69-79(1994).

[10] *E. Ahmed, A.S. Elgazzar*, On fractional order differential equations model for nonlocal epidemics, Physica A,**379**, 607-614(2007).

[11] *S. Gakkhar, N. Chavda*, A dynamical model for HIV–TB co-infection, Appl. Math. Comput.,**280,** 9261–9270(2012).

[12] *A.S. Waziri, E.S. Massawe, O.D. Makinde*, Mathematical modelling of HIV/AIDS dynamics with treatment and vertical transmission, Appl. Math.,**2**, 77–89(2012).

[13] M. *Pitchaimani, C. Monica and M. Divya*, Stability analysis for HIV infection delay model with protease inhibitor, BioSystems,**114**, 118–124 (2013).

[14] *E. A. Hernandez-Vargas and R.H. Middleton,* Modeling the three stages of HIV infection, J. Theor. Biol., **320**, 33–40 (2013).

[15] *C.M.A. Pinto and A.R.M. Carvalho*, Mathematical model for HIV dynamics in HIV-specific helper cells, Commun. Nonlin. Sci,.**19**, 693–701 (2014).

[16] *C.M.A. Pinto, A.R.M. Carvalho*, New findings on the dynamics of HIV and TB coinfection models, Applied Mathematics and Computation,**242,** 36-46(2014).

[17] *C.M.A. Pinto, A.R.M. Carvalho*, Fractional modeling of typical stages in HIV epidemics with drug-resistance, Progr. Fract. Differ. Appl. **1 (2)**, 111-122(2015).

[18] *B.N. Mandal, S. Bhattacharya*, Numerical solution of some classes of integral equations using Bernstein polynomials, Applied Mathematics and Computation, **190,** 1707-1716(2007).

[19] *S.A. Yousefi, M. Behrooozifar*, Operational matrices of Bernstein polynomials and their applications, International Journal of System Science, **41,**709-716(2010).

[20] *M. Alipour, D. Rostamy, and D. Baleanu*, Solving multidimensional FOCPs with inequality constraint by BPs operational matrices, Journal of Vibration and Control, 2012, DOI:10.1177/1077546312458308.

[21] *D. Rostamy, M. Alipour, H. Jafari, and D. Baleanu*, Solving multi-term orders fractional differential equations by operational matrices of BPs with convergence analysis, Romanian Reports in Physics, **65 (2),** 334-349(2013).

[22] *H. Khan, M. Alipour, H. Jafari, R. Ali Khan*, Approximate analytical solution of a coupled system of fractional partial differential equations by Bernstein polynomials, International Journal of Applied and Computational Mathematics, 2015, DOI 10.1007/s40819-015-0052-8.

[23] *A.A. Kilbas, H.M. Srivastava, J.J. Trujillo*, Theory and applications of fractional differential equations. In: North-Holland mathematics studies, vol 204. Elsevier Science B.V., Amsterdam, 2006.

[24] *C. Canuto, M.Y. Hussaini, A. Quarteroni, T.A. Zang*, Spectral Methods in Fluid Dynamic, Prentice-Hall, Englewood Cliffs, NJ, 1988.